The Absence of Indoleamine 2,3-Dioxygenase Inhibits Retinal Capillary Degeneration in Diabetic Mice

Rooban B. Nahomi,[1,2] Sruthi Sampathkumar,[1] Angela M. Myers,[3] Lynda Elghazi,[3] Dawn G. Smith,[1] Jie Tang,[4] C. Allen Lee,[4] Timothy S. Kern,[1,4] Ram H. Nagaraj,[1,2] and Patrice E. Fort[3]

[1]Departments of Ophthalmology and Visual Sciences, Case Western Reserve University School of Medicine, Cleveland, Ohio, United States
[2]Department of Ophthalmology, University of Colorado School of Medicine, Aurora, Colorado, United States
[3]Kellogg Eye Center, Department of Ophthalmology and Visual Sciences, University of Michigan, Ann Arbor, Michigan, United States
[4]Medicine, Case Western Reserve University School of Medicine, Cleveland, Ohio, United States

PURPOSE. Loss of retinal capillary endothelial cells and pericytes through apoptosis is an early event in diabetic retinopathy (DR). Inflammatory pathways play a role in early DR, yet the biochemical mechanisms are poorly understood. In this study, we investigated the role of indoleamine 2,3-dioxygenase (IDO), an inflammatory cytokine-inducible enzyme, on retinal endothelial apoptosis and capillary degeneration in the diabetic retina.

METHODS. IDO was detected in human and mouse retinas by immunohistochemistry or Western blotting. Interferon-γ (IFN-γ) levels were measured by ELISA. IDO levels were measured in human retinal capillary endothelial cells (HREC) cultured in the presence of IFN-γ ± 25 mM D-glucose. Reactive oxygen species (ROS) were measured using CM-H$_2$DCFDA dye and apoptosis was measured by cleaved caspase-3. The role of IDO in DR was determined in IDO knockout (IDO$^{-/-}$) mice with streptozotocin-induced diabetes.

RESULTS. The IDO and IFN-γ levels were higher in human diabetic retinas with retinopathy relative to nondiabetic retinas. Immunohistochemical data showed that IDO is present in capillary endothelial cells. IFN-γ upregulated the IDO and ROS levels in HREC. The blockade of either IDO or kynurenine monooxygenase led to inhibition of ROS in HREC. Apoptosis through this pathway was inhibited by an ROS scavenger, TEMPOL. Capillary degeneration was significantly reduced in diabetic IDO$^{-/-}$ mice compared to diabetic wild-type mice.

CONCLUSIONS. The results suggest that the kynurenine pathway plays an important role in the inflammatory damage in the diabetic retina and could be a new therapeutic target for the treatment of DR.

Keywords: IFN-γ, indoleamine 2,3-dioxygenase, retinal endothelial cells, apoptosis, diabetic retinopathy, acellular capillaries

Diabetic retinopathy (DR) is the most common cause of visual impairment in industrialized countries.[1] With 79 million people in the United States satisfying the criteria for prediabetes, the prevalence of DR is predicted to increase manifold in the coming years. The exact series of events involved in the pathogenesis of retinal vascular, neuronal, and glial dysfunction in DR remains elusive.

Chronic retinal inflammation resulting from hyperglycemia is associated with the onset and progression of early DR.[1–3] Inflammatory cytokines such as TNF-α, IL-1β, IL-6, and interferon-γ (IFN-γ) are elevated in the blood, retina, vitreous, and aqueous humor of diabetics,[4–10] causing an imbalance between proapoptotic and prosurvival signals.[11] Capillary cell death occurs in the presence of elevated cytokines.[12,13] Although TNF-α, IL-1β, and IL-6 are strongly associated with DR, very little is known about the role of IFN-γ in the pathogenesis of DR.

IFN-γ is a pleiotropic, dimeric soluble cytokine that is mainly secreted by T-helper 1 cells, cytotoxic T cells, dendritic cells, and natural killer cells. It promotes macrophage, B-cell, and T-cell activation.[14–16] IFN-γ is elevated in the serum and eyes of patients with diabetes, in diabetic rat retinas, and in the vitreous of patients with proliferative vitreoretinopathy (PVR), uveitis, and other inflammatory ocular conditions.[17–20] IFN-γ inhibits proliferation and tube formation in human umbilical vein endothelial cells,[21] induces endothelial cell apoptosis, and inhibits neovascularization in a metastatic brain tumor mouse model.[22] Notably, IFN-γ is the most potent known inducer of indoleamine 2,3-dioxygenase (IDO).[23,24]

IDO is primarily produced by activated macrophages[25] and certain tumor cells.[26] It is the key regulatory enzyme in the kynurenine pathway and initiates the oxidative cleavage of L-tryptophan (L-Trp) to N-formyl kynurenine (Nfk).[27] Nfk is converted to NAD$^+$ through a series of intermediates, which include kynurenine (Kyn) and 3-hydroxy kynurenine (3OH-Kyn).[28] Kyn is formed from Nfk through the action of kynurenine formamidase, and 3OHKyn is formed from Kyn through kynurenine monooxygenase (KMO), which is a mitochondrial NADPH-dependent enzyme.[29] Kynurenine pathway intermediates can induce apoptosis in a number of cell

types.[30] Our previous work has linked Kyn with G2/M cell cycle arrest[31] and 3OHKyn with lens epithelial cell apoptosis in vitro.[32] The purpose of this study was to determine whether IFN-γ induces IDO expression in human retinal endothelial cells (HREC) and to determine the role of IDO in an experimental model of DR. When this work was in progress, Hu et al.[33] published a paper that showed higher levels of IDO in human and rat diabetic retinas when compared to nondiabetic retinas. In flat-mount retinas IDO was shown to be localized primarily in microglia in that study.

METHODS

Tissue Samples

Eyes were obtained from 17 diabetic (both T1 or T2) donors (average age = 64 years, range, 54–74 years) and 11 nondiabetic donors (average age = 64 years, range, 53–74 years) within 8 to 10 hours of death from the Midwest Eye Bank (now Eversight) in Ann Arbor, Michigan, United States. This study was carried out in accordance with the recommendations of the Declaration of Helsinki. The diabetic donors were split between those without any signs of DR and those with mild retinopathy (few microaneurysms), as demonstrated by fundus photograph and optical coherence tomography. The duration of diabetes ranged from 2 to 40 years and the hemoglobin A1c (HbA1c) levels ranged from 5.5% to 9.7%. There were no significant differences in either duration or HbA1c levels between diabetic donors with and without retinopathy. The groups consisted predominantly of Caucasians and females. Neither diabetic nor nondiabetic donors had any significant ocular history other than cataract surgery.

Immunohistochemistry

Ocular globes were dissected and processed by sequential incubation in a sucrose gradient before being embedded in a mix of OCT (optimal cutting temperature) compound (Tissue-Tek, Torrance, CA, USA) and 20% sucrose (1:1). Eight-micrometer-thick sections were prepared and permeabilized in a solution of 0.3% Triton X-100 and blocking in 3% normal donkey serum + 1% BSA. The sections were rinsed briefly in PBS and incubated with antibodies to IDO (mouse monoclonal, 1:200 dilution; Millipore, Billerica, MA, USA; Cat. No. MAB5412), PECAM-1 (rabbit polyclonal, 1:200 dilution; Cell Signaling, Danvers, MA, USA; Cat. No. 77699), and CD-34 (rabbit monoclonal, 1:200 dilution; Abcam, Cambridge, MA, USA; Cat. No. ab81289) in blocking buffer. The sections were then incubated with appropriate secondary antibodies conjugated with either Texas Red or Oregon Green (Invitrogen, Carlsbad, CA, USA), rinsed, and permanently mounted with 4′,6-Diamidino-2-Phenylindole (DAPI; Vector Laboratories, Burlingame, CA, USA). Images were acquired using a Leica (Buffalo Grove, IL, USA) confocal SP5 microscope with a ×40 objective.

Cell Culture and Treatment

HREC were isolated and cultured as previously described.[34] The purity of isolation was 95% to 99%, as determined by PECAM-1 staining and DiI-Ac-LDL (Biomedical Technologies, Tewksbury, MA, USA) uptake (Figs. 1A, 1B). The cells used in all experiments were between passages 3 and 8. HREC were cultured on 0.2% gelatin-coated plates in medium containing Dulbecco's modified Eagle's medium (DMEM)/F12 (1:1 ratio) supplemented with 10% fetal bovine serum, 15 μg/mL endothelial cell growth supplements (Sigma-Aldrich Corp.,

St. Louis, MO, USA), 1% penicillin/streptomycin, and 1% insulin/transferrin and selenium (Sigma-Aldrich Corp.) at 37°C in a humidified atmosphere containing 95% air and 5% CO_2. The medium was changed every 48 hours.

For cytokine treatment, HREC were incubated with 1 to 5 U/mL IFN-γ (R&D Systems, Inc., Minneapolis, MN, USA), 10 ng/mL TNF-α (Invitrogen, Grand Island, NY, USA) or 10 ng/mL IL-1β (Invitrogen) with or without 25 mM D-glucose for 48 hours in serum-free media. Cells grown in the presence of 20 mM D-mannitol or L-glucose (total glucose = 25 mM) were used as osmotic and metabolic controls, respectively. In some experiments, cells were exposed to 20 μM 1-methyl D, L-tryptophan (MT, Sigma-Aldrich Corp.) to inhibit IDO or 50 μM Ro61-8048 (Tocris Bioscience, Minneapolis, MN, USA) to inhibit KMO. To determine the role of reactive oxygen species (ROS), cells were incubated with 100 μM TEMPOL (Sigma-Aldrich Corp.), a cell-permeable ROS scavenger.

Measurement of IDO Activity

HREC were lysed with M-PER (Thermo Scientific, Waltham, MA, USA) containing a diluted protease inhibitor cocktail (1:100) and centrifuged at 14,000*g* for 10 minutes, and the supernatant was separated. The supernatant protein concentration was measured using the bicinchoninic acid assay method with a BSA standard. Lysate from HREC was incubated with a reaction mixture (50 mM sodium phosphate buffer [pH 6.5], 20 mM ascorbic acid sodium salt, 200 μg/mL bovine pancreatic catalase, 10 μM methylene blue, and 400 μM L-Trp) at 37°C for 1 hour. After stopping the reaction with 30% trichloroacetic acid, the samples were incubated at 65°C for 15 minutes followed by centrifugation at 20,000*g*. The supernatant was analyzed by C18-RP HPLC against a Kyn standard.[32] One IDO unit is defined as one nmol Kyn formed/mg protein/h.

SDS-PAGE and Western Blotting

Lysates of HREC were resolved by SDS-PAGE (12%), electrophoretically transferred to a nitrocellulose membrane, blocked with 5% non-fat dry milk in Tris Buffered Saline with Tween 20 (NFDM/TBST), and incubated overnight with an antibody against IDO (Millipore, 1:1000 dilution) or β-actin (Cell Signaling; Cat. No. 4970, 1:5000 dilution), each diluted in 5% NFDM/TBST. Appropriate horseradish peroxidase (HRP)-conjugated secondary antibodies were used. Proteins were detected using the SuperSignal West Pico or Femto Kit (Pierce Chemicals, Dallas, TX, USA). For IDO Western blotting in retinas, tissues from diabetic (5 months) and age-matched S129 mice strain were sonicated with 1× radioimmunoprecipitation assay (RIPA) buffer containing protease inhibitor cocktail (1:100). Protein at concentration of 40 μg was loaded on 4% to 12% gradient gel. Membranes were blocked with 5% NFDM/TBST after wet transfer, then incubated overnight with IDO (1:500 dilution) or β-actin (Millipore; Cat. No. 1501, 1:5000 dilution). Images were captured by GE Typhoon FLA 9000 (Pittsburgh, PA, USA).

Measurement of IDO mRNA by Quantitative PCR

Total RNA was extracted from the cultured HREC using the RNeasy Plus Mini Kit (Qiagen, Redwood City, CA, USA). RNA was reverse transcribed to generate cDNA using the QuantiTect Reverse Transcription Kit (Qiagen). Quantitative PCR with SYBR green detection was performed using a Bio-Rad iCycler IQ thermocycler (Billerica, MA, USA) with the following sets of primers: IDO, 5′ GCA AAT GCA AGA ACG GGA CAC T (sense) and 5′ TCA GGG AGA CCA GAG CTT TCA CAC (antisense), and
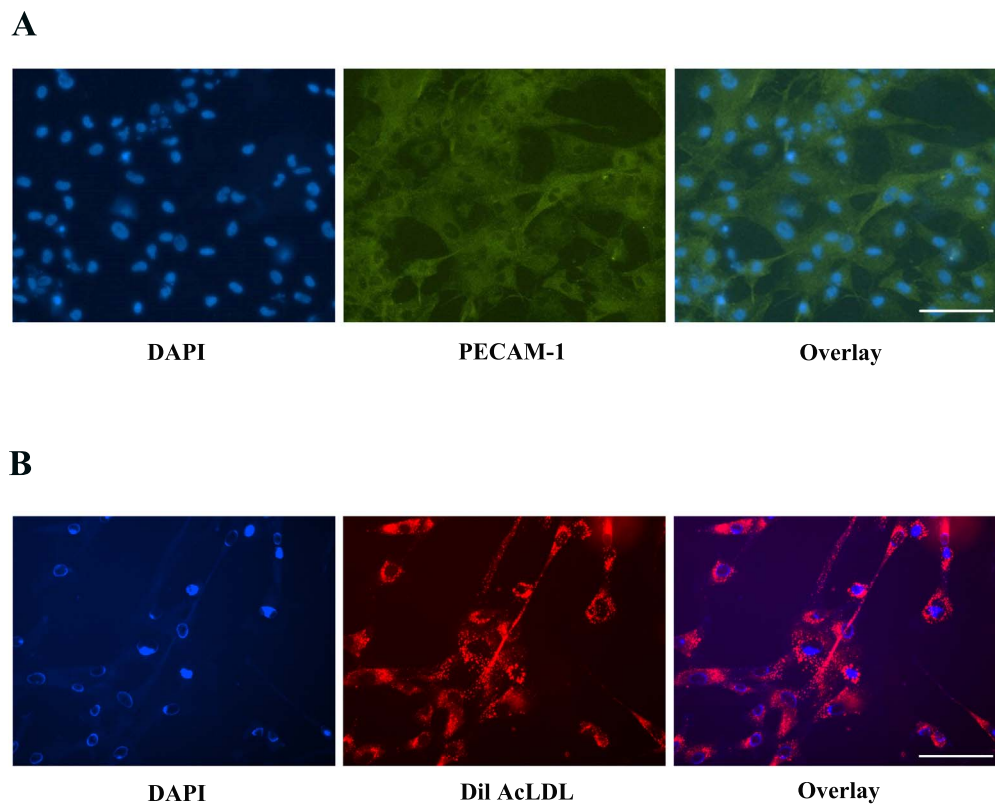
A

DAPI   PECAM-1   Overlay

B

DAPI   DiL AcLDL   Overlay

FIGURE 1.   Characterization of isolated HREC. Isolated HREC were characterized by (**A**) PECAM-1 immunostaining and (**B**) an assay of DiL-Ac-LDL uptake. The images are representative of three independent experiments. *Scale bar*: 100 μm.

β-actin, 5′ AGG CAC CAG GGC GTG AT (sense) and GCC CAC ATA GGA ATC CTT CTG AC (antisense).

ELISA for IFN-γ

The contralateral eyes from diabetic and nondiabetic donors used for the immunohistochemistry experiments were dissected at the time of recovery. Individual ocular tissues, including the peripheral retinas, were rapidly frozen on dry ice before storage at −80°C until processing. A piece of nonfixed peripheral retina was isolated and homogenized by sonication in 150 μL M-PER buffer. Mouse retinas were processed similarly with 100 μL M-PER buffer. Whole blood was collected from diabetic and nondiabetic mice. Serum was separated and stored at −80°C until analysis. IFN-γ was quantified using the OptEIA Human or Mouse IFN-γ ELISA Kit (BD Biosciences, San Jose, CA, USA) per the manufacturer's instructions.

Assessment of Cell Viability

The ability of HREC to bioreduce a tetrazolium compound (3-[4,5-dimethylthiazol-2-yl]-5-[3-carboxymethoxyphenyl]-2-[4-sulfophenyl]-2H-tetrazolium, inner salt; MTS from Sigma-Aldrich Corp.) in the mitochondria was measured by determining the formation of a colored formazan compound via spectrophotometric detection at 570 nm. The number of viable cells per well in 96-well plates was calculated from a standard curve that was obtained using 0 to 1000 HREC/well.

ROS Determination

ROS generation was measured by fluorescence microscopy using CM-H$_2$DCFDA (Molecular Probes, Eugene, OR, USA). The fluorescence intensity emitted by HREC grown in 48-well plates was measured using Meta Morph software (Molecular Devices, San Jose, CA, USA) and is represented by a bar graph.

Detection of Apoptosis

The number of apoptotic and viable HREC in randomly selected areas/well of a 48-well plate was determined by staining with Hoechst 33342 reagent (Life Technologies, Grand Island, NY, USA). Approximately 300 cells were counted in each group. The percentage of apoptotic cells relative to the total number of cells was calculated. In addition, we measured cleaved caspase-3 by Western blotting using a specific antibody (Cell Signaling; Cat. No. 9664, 1:1000 dilution) as mentioned above.

Induction of Diabetes in Mice and Assessment of Retinal Capillary Degeneration

All animal experiments were performed under strict adherence to the ARVO Statement for the Use of Animals in Ophthalmic and Vision Research and in accordance with the institutional guidelines. IDO knockout (IDO$^{-/-}$) and wild-type (WT) mice (all on C57BL/6J background) were obtained from Jackson Laboratories (Bar Harbor, ME, USA). Male IDO$^{-/-}$ and WT mice at 3 months of age were administered five sequential intraperitoneal injections of streptozotocin (MP Biomedicals, Solon, OH, USA) solution freshly prepared in citrate buffer (pH 4.5) at a dose of 55 mg/kg body weight on 5 consecutive days (to animals fasted for 6 hours) to induce diabetes. Neutral protamine hagedorn (NPH) insulin (0.2 units) was administered subcutaneously up to three times a week to prevent weight loss. After 8 months of diabetes, animals were killed for biochemical and histopathologic studies. Retinal capillary bed preparation
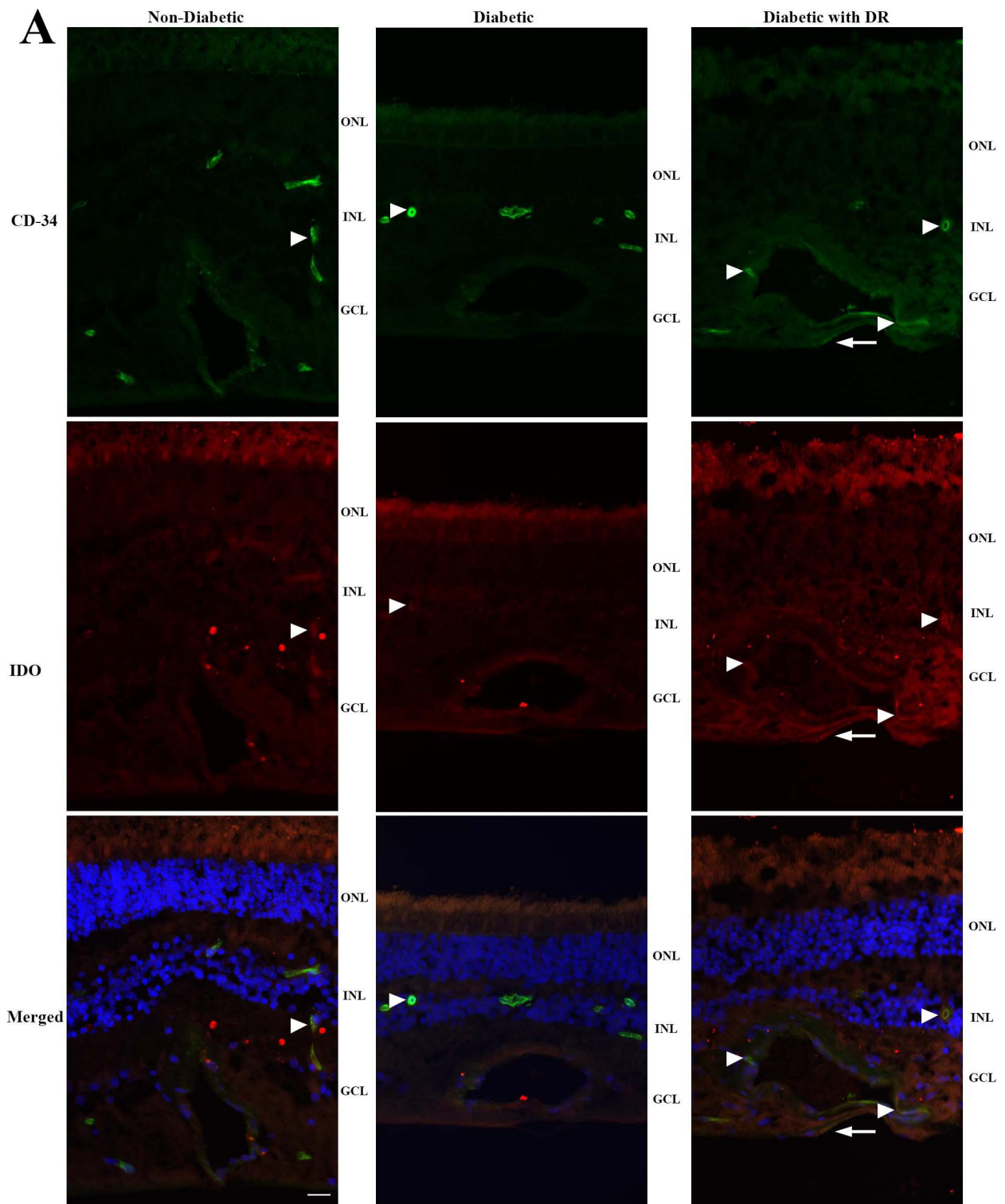
FIGURE 2. IFN-γ and IDO expression are elevated in human diabetic retinas. (**A**) Immunohistochemistry of retinal sections shows IDO (*red*) colocalizing with CD-34 (*green*) in the capillary endothelium (*arrowheads*) of the retina of diabetic donors with retinopathy (*right*). IDO-positive staining was also observed in the capillary endothelium of the retina of diabetic donors without retinopathy (*middle*) and nondiabetic donors (*left*), but the signal appears diffuse and less intense (*arrowheads*). Additionally, some of the IDO signal in the inner retina of diabetic donors with retinopathy appears not to colocalize with CD-34 (*arrows*), suggesting expression in other cells of the retina. Nuclei are stained with DAPI (*blue*). (**B**) IFN-γ levels were measured by ELISA in retinal homogenates from age-matched nondiabetic (*n* = 9), diabetic (without retinopathy, *n* = 8), and diabetic (with retinopathy, *n* = 7) donors. *Scale bar*: 20 μm. *P* < 0.05; NS, not significant.
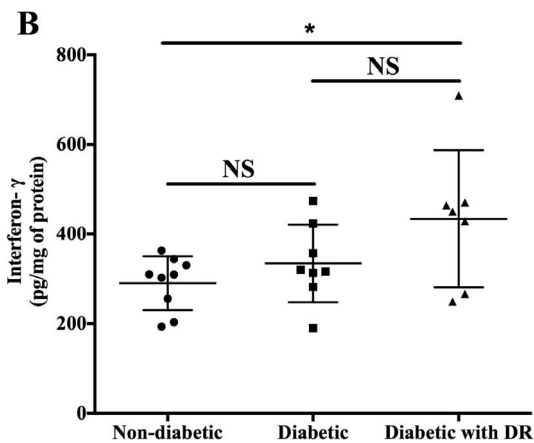
FIGURE 2. Continued.

and a blinded quantification of degenerated capillaries were performed as described previously.[35] Briefly, whole eyes were fixed and digested with elastase for 1.5 hours at 37°C in an agitating water bath after washing with water for overnight. Following enzymatic digestion, eyes were washed with 100 mM Tris-HCl pH 8.5 for overnight, and isolated vasculature was laid on a glass microscopic slide. This was dried overnight and stained with hematoxylin and periodic acid Schiff.

Statistics

The data were analyzed using StatView software (v.5.0.1; SAS Institute, Inc., Cary, NC, USA) and are presented as the mean ± SD of the specific number of experiments indicated in the figure legends. Statistical significance was evaluated using ANOVA followed by Fisher's protected least significant difference test. The differences were considered significant at $P < 0.05$.

RESULTS

Diabetes Leads to Increased IFN-γ and IDO Levels in Human Retinas

In nondiabetic retinas, immunostaining revealed a faint and diffuse staining for IDO that colocalizes with CD-34, a marker of the retinal blood vessels. Immunostaining of retinas from diabetic donors also revealed a colocalization of IDO and CD-34, with a noticeably more defined and intense IDO-positive signal in retinal tissues of diabetic donors with retinopathy, suggesting the induction of IDO in the retinal capillary endothelium of DR patients (Fig. 2A, arrowheads). Of note, positive IDO signal was also detected in nonvascular cells of the ganglion cell layer (Fig. 2A, arrows). To quantify the impact of diabetes on IFN-γ, an ELISA was used to measure it in peripheral retinal lysates of diabetic donors with and without DR, as well as matched nondiabetic human donors. Interestingly, while only a trend toward higher levels could be observed in diabetic donors without retinopathy, a 50% increase in the IFN-γ levels ($P < 0.05$) was observed in the retina of diabetic donors with retinopathy relative to retinas from age-matched nondiabetic donors (Fig. 2B).

Consistent with the human data reported above, Western blotting analysis of IDO in the mouse retinal homogenates shows higher IDO content in the diabetic retina when compared to the nondiabetic retina. (Fig. 3A). We would like to point out that there were two protein bands for IDO in both
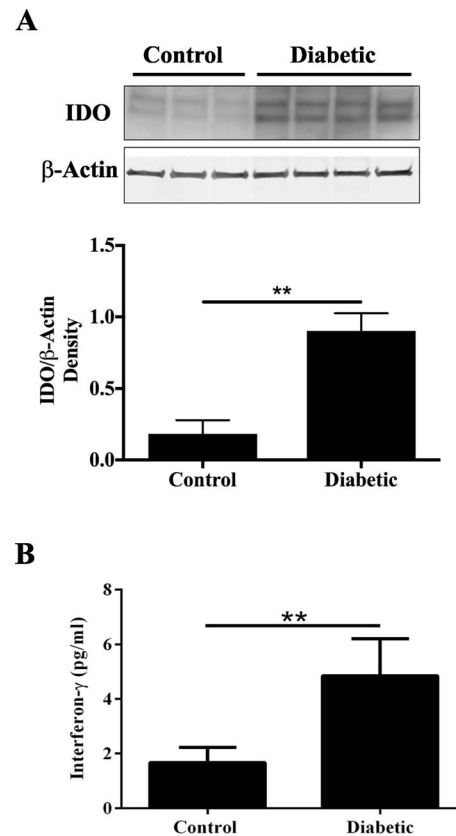

FIGURE 3. IDO is upregulated in retinas of diabetic mice along with systemic elevation of IFN-γ. (A) Western blotting for IDO protein content (39 and 43 kDa) in mouse diabetic and nondiabetic retinas. (B) The diabetic WT mice showed significantly increased levels of IFN-γ in the serum when compared with nondiabetic controls, $n = 5$. **$P < 0.005$.

diabetic and nondiabetic retinas. While the band at 43 kDa is the expected one for IDO, the band at 39 kDa could be a splice variant or post-translationally modified protein. However, additional work, possibly mass spectrometric analysis, could confirm that the protein bands are two variants of IDO. Diabetic mice showed a 2.5-fold increase in serum IFN-γ levels compared to nondiabetic controls (Fig. 3B). The mouse retinal IFN-γ levels were extremely low when compared to those in humans, and there was no difference between diabetic and nondiabetic mouse retinas (Supplementary Fig. S1).

HG Enhances IFN-γ–Mediated IDO Upregulation in HREC

HREC were treated with varying concentrations of IFN-γ in the presence or absence of High Glucose (HG; 25 mM D-glucose). With HG, the induction of IDO by 2 and 5 U/mL IFN-γ was approximately 20% and 30% higher, respectively, than without HG (Figs. 4A, 4B). With 5 U/mL IFN-γ and HG, we found a 25% increase in IDO mRNA expression compared to that in cells without HG (Fig. 4C). In the absence of IFN-γ, HG alone slightly increased IDO expression but it was not statistically significant (Fig. 4C, inset). Osmotic (20 mM mannitol + 5 mM D-glucose) and metabolic (20 mM L-glucose + 5 mM D-glucose) controls in the presence of IFN-γ did not influence the IDO content similar to HG (Fig. 4D) or the activity (Fig. 4E). Neither TNF-α nor IL-1β had an inducible effect on IDO (Fig. 4F).
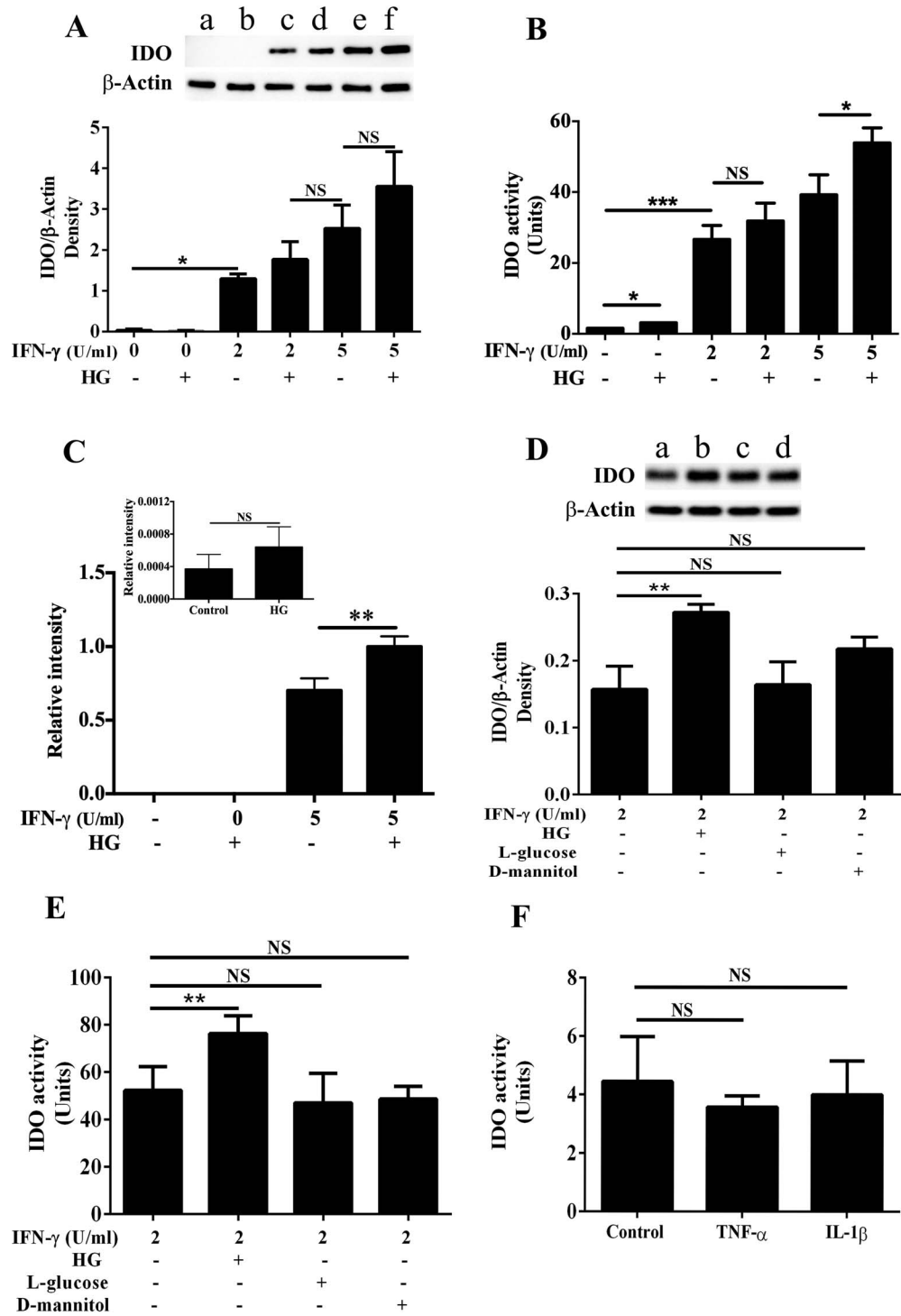
FIGURE 4. HG enhances the dose-dependent activation of IDO by IFN-γ in HREC. HREC were treated with 0, 2, and 5 U/mL IFN-γ in the presence or absence of HG for 48 hours. IFN-γ dose-dependently induced (**A**) IDO protein expression (43 kDa), (**B**) IDO activity, and (**C**) IDO mRNA (normalized to β-actin) levels. HG further enhanced the effects of IFN-γ on IDO expression and IDO activity. In (**C**) (*inset*), HG alone showed a slight but statistically insignificant increase in IDO. **a**, Control; **b**, HG alone; **c**, 2 U/mL IFN-γ; **d**, 2 U/mL IFN-γ + HG; **e**, 5 U/mL IFN-γ; **f**, 5 U/mL IFN-γ + HG. D-mannitol or L-glucose did not have similar effects on either (**D**) IDO content or (**E**) IDO activity. **a**, 2 U/mL IFN-γ; **b**, 2 U/mL IFN-γ + HG; **c**, 2 U/mL IFN-γ + L-glucose; **d**, 2 U/mL IFN-γ + D-mannitol. (**F**) IDO activity in HREC was unaffected by 10 ng/mL each of TNF-α and IL-1β treatment (48 hours) compared with untreated controls. The Western blots in (**A, D**) are from representative samples in each group. The *bars* are the mean ± SD of three independent experiments. *$P < 0.05$; **$P < 0.005$; ***$P < 0.0005$; NS, not significant.
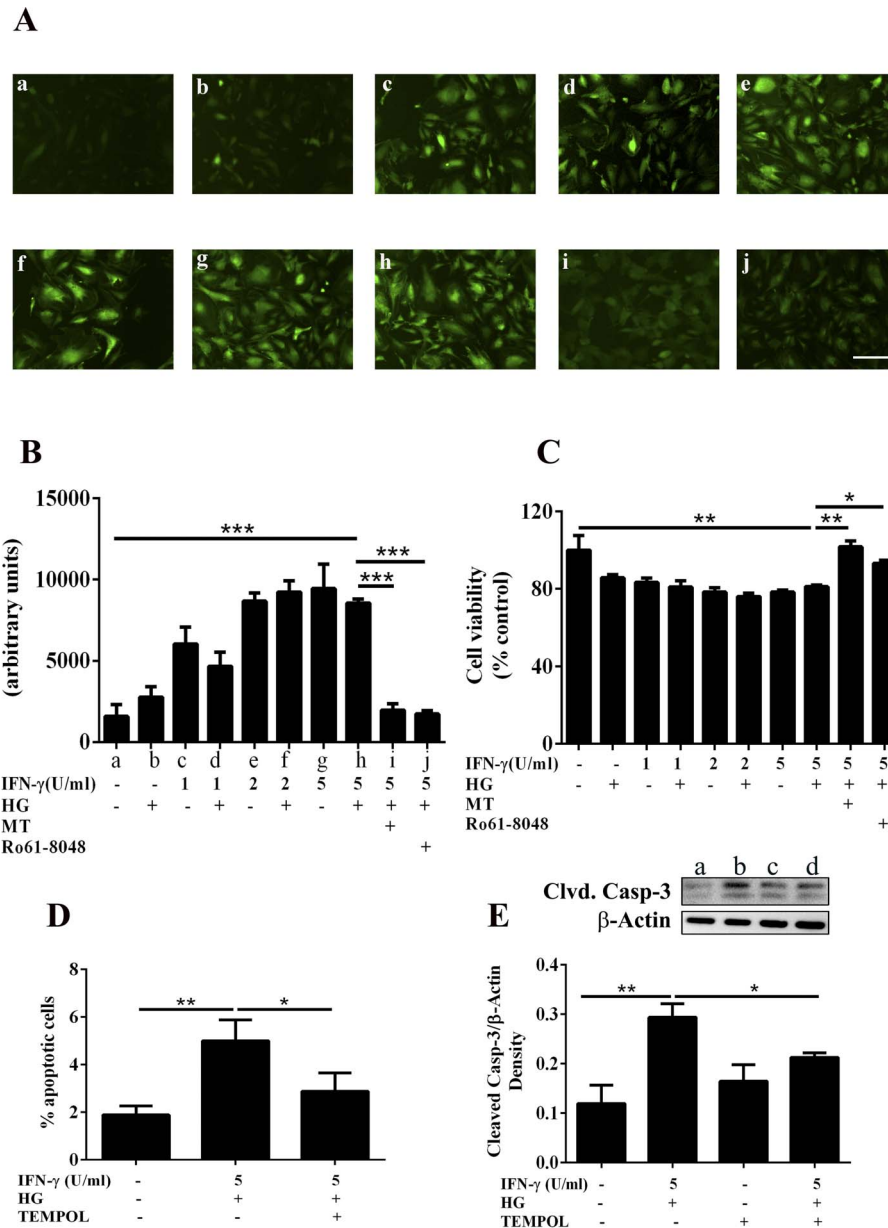
FIGURE 5. Activation of IDO by IFN-γ and HG leads to oxidative stress and reduces the viability of HREC. (A) Intracellular ROS generation was detected by fluorescence microscopy after probing with CM-H$_2$DCFDA. MT and Ro61-8048 blocked ROS generation in HREC treated with IFN-γ and HG. **a**, Control; **b**, HG alone; **c**, 1 U/mL IFN-γ; **d**, 1 U/mL IFN-γ + HG; **e**, 2 U/mL IFN-γ; **f**, 2 U/mL IFN-γ + HG; **g**, 5 U/mL IFN-γ; **h**, 5 U/mL IFN-γ + HG; **i**, 5 U/mL IFN-γ + HG + MT; **j**, 5 U/mL IFN-γ + HG + Ro61-8048; *scale bar*: 50 μm. (B) The fluorescence intensity corresponding to ROS levels was measured and is shown in the bar graph. The letters in lowercase within photomicrographs in (A) correspond to bars in the graph. (C) The treatment of HREC with IFN-γ and HG caused a reduction in the number of viable cells as determined by an MTT assay. This was blocked by treatment with MT or Ro61-8048. (D, E) Treatment with TEMPOL, a cell-permeable antioxidant, ameliorated caspase-3–mediated apoptosis in the IFN-γ– and HG-treated HREC. **a**, Control; **b**, 5 U/mL IFN-γ + HG; **c**, TEMPOL alone; **d**, 5 U/mL IFN-γ + HG + TEMPOL. The *bars* in (**B**–**E**) are the mean ± SD of three independent experiments. *$P < 0.05$; **$P < 0.005$; ***$P < 0.0005$. Clvd Casp-3 or Cleaved Casp-3, cleaved caspase-3.

Downstream Metabolic Products of IDO Reduce the Viability of HREC and Promote Apoptosis by Oxidative Stress

Kynurenines, primarily 3OHKyn, generate ROS.[36,37] Cultured HREC were probed with CM-H$_2$DCFDA, a cell-permeable dye that fluoresces after oxidation by ROS. The ROS content in HREC increased with IFN-γ concentration. MT (IDO inhibitor) and Ro61-8048 (KMO inhibitor) significantly reversed ROS production (Figs. 5A, 5B). IFN-γ decreased the number of viable cells in the presence of HG (Fig. 5C), while cotreatment with MT or Ro61-8048 reversed this effect. Consistently, we found that nearly 5% of the cells were apoptotic when treated with 5 U/mL IFN-γ + HG. TEMPOL, a cell-permeable free radical scavenger,[38] blocked IFN-γ–induced caspase-3–mediated apoptosis in HREC, supporting the central role of ROS in this process (Figs. 5D, 5E).

Retinal Capillary Degeneration Is Reduced in IDO$^{-/-}$ Diabetic Mice

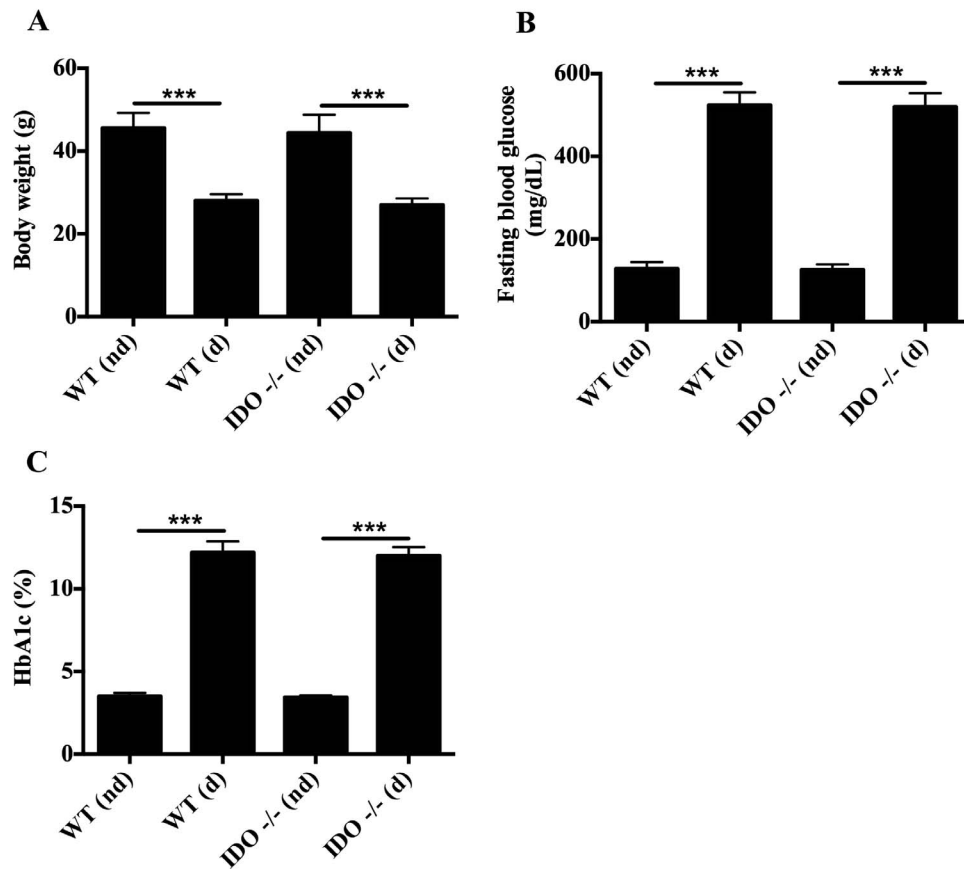WT and IDO$^{-/-}$ mice were made diabetic by intraperitoneal streptozotocin injections. All diabetic mice, whether they

A

B

C

FIGURE 6. Diabetic mice lacking IDO show reduced retinal capillary degeneration. (**A**) Diabetic mice had lower body weights, (**B**) higher fasting blood glucose levels, and (**C**) higher HbA1c levels when compared to nondiabetic mice. (**D**) Flat mounts of retinas stained with hematoxylin and periodic acid Schiff. Capillary cell degeneration is reduced in diabetic IDO$^{-/-}$ mice relative to diabetic WT mice. (**E**) Degenerated acellular capillaries (indicated by *arrows*) were quantified and are represented as a bar graph. *Bars* are the mean ± SD of three independent values. ***$P < 0.0005$. d, diabetic; nd, nondiabetic.

expressed IDO or not, had lower body weights (Fig. 6A) and higher fasting blood glucose levels (Fig. 6B) compared to nondiabetic mice, and diabetic mice had glycated hemoglobin levels of 12.5% (Fig. 6C). The mortality rate in diabetic mice was ∼20% compared to 0% in nondiabetic WT and IDO$^{-/-}$ mice. Diabetic (WT) animals exhibited a significantly higher number of acellular capillaries relative to nondiabetic controls (Figs. 6D, 6E).

DISCUSSION

The diabetic retina shows evidence of dysregulated proinflammatory factors, such as IL-1α, IL-1β, IL-6, IFN-γ, and TNF-α, as well as leukostasis and microglial activation.[1,39,40] Various inflammatory pathways act as key mediators in the development and progression of DR. In the present study, we focused on IDO, an IFN-γ–inducible enzyme of the Kyn pathway. We hypothesized that if IFN-γ was upregulated in diabetic retina, it would promote IDO synthesis with potential cellular implications. To verify this hypothesis, we measured the IFN-γ levels in human retinas. IFN-γ was increased by 50% in diabetic retinas (with retinopathy) when compared to nondiabetic samples. Next, we checked whether the elevated IFN-γ affected IDO in diabetic retinas by immunohistochemistry. Retinal sections from diabetic donors were intensely labeled for IDO with colocalization in the retinal vascular endothelium. These observations point to a direct role of IFN-γ in the promotion

of IDO synthesis in human diabetic retinas. The higher expression of IDO in diabetic mouse retinas in the absence of elevated IFN-γ is difficult to explain, but points to the possibility of other factors that could promote IDO synthesis.

At present, the source of IFN-γ in the retina is unclear. Although T cells and natural killer (NK) cells are considered major sources of IFN-γ, microglial cells have also been shown to produce IFN-γ.[41,42] It is possible that elevated retinal IFN-γ in diabetes could be from microglia and possibly from T cells if they infiltrate the retina. In support of the microglial origin of IFN-γ, Hu et al.[33] recently showed that IDO is present in human retinal microglial cells and its levels are increased in diabetic human and rat retinas.

Even though we were not able to measure human serum IFN-γ levels, there is much evidence that points to elevated IFN-γ levels in diabetes.[43–45] We observed a 2.5-fold increase in serum IFN-γ levels in diabetic mice relative to nondiabetic mice. Whether elevated serum IFN-γ in diabetes has an effect on retinal IDO expression needs to be investigated.

We found that in the diabetic retina, IDO was primarily expressed in the retinal capillary endothelium and proposed that IFN-γ could promote IDO expression in those cells. We then tested how hyperglycemia affects IFN-γ–mediated IDO induction in HREC. IDO mRNA expression and protein content and activity were elevated in cells exposed to high glucose plus IFN-γ compared to cells incubated in normal glucose plus IFN-γ. Thus, in an uncontrolled diabetes-like environment (25 mM
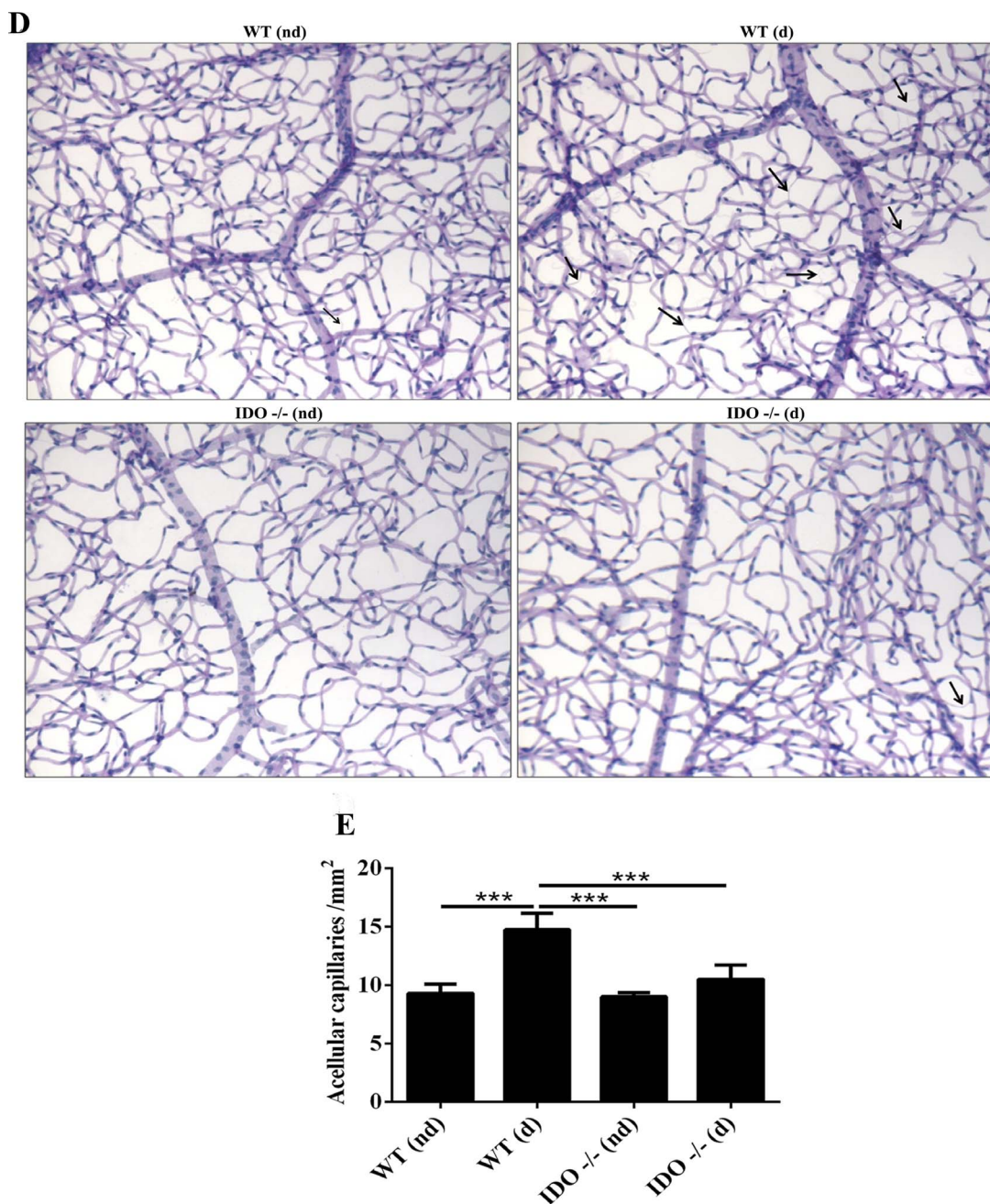
D

WT (nd) | WT (d) | IDO -/- (nd) | IDO -/- (d)

E

FIGURE 6. Continued.

D-glucose is equivalent to ∼450 mg/dL blood glucose), hyperglycemia would potentiate IDO induction by IFN-γ. Further, IFN-γ induced IDO expression and activity in a dose-dependent manner. Other proinflammatory cytokines such as TNF-α and IL-1β also potentiate IFN-γ–mediated IDO induction.[46,47] Whether such a synergy occurs in HREC remains to be verified. We found that TNF-α and IL-1β alone failed to induce IDO in HREC. Unlike our study with retinal sections, the study by Hu et al.[33] used flat mounts of human and rat retinas for IDO detection. That study detected IDO in microglial cells, and higher levels in diabetic than nondiabetic retinas. Thus, diabetes could elevate IDO levels in both retinal vasculature and microglia and contribute to neurovascular damage.

De novo biosynthesis of nicotinamide adenine dinucleotide (NAD^+) through the Kyn pathway produces several kynurenines with redox potential; that is, these metabolites can donate or accept electrons. Of the various metabolites, Kyn is implicated in worsening insulin resistance, and 3OHKyn is implicated in endothelial dysfunction, generation of free radicals, and cellular apoptosis.[48-51] Under physiological conditions, a state of redox balance exists in the pathway. Increased IDO activity in diabetes causes an imbalance, with ROS overriding the antioxidant and mitochondrial protective mechanisms to cause oxidative stress. We tested if this was true in HREC and found that in cells exposed to IFN-γ plus high glucose, the generation of ROS was high. This oxidative stress was associated with reduced viability of HREC and an increase in apoptosis. Blocking the IDO with MT or the KMO with
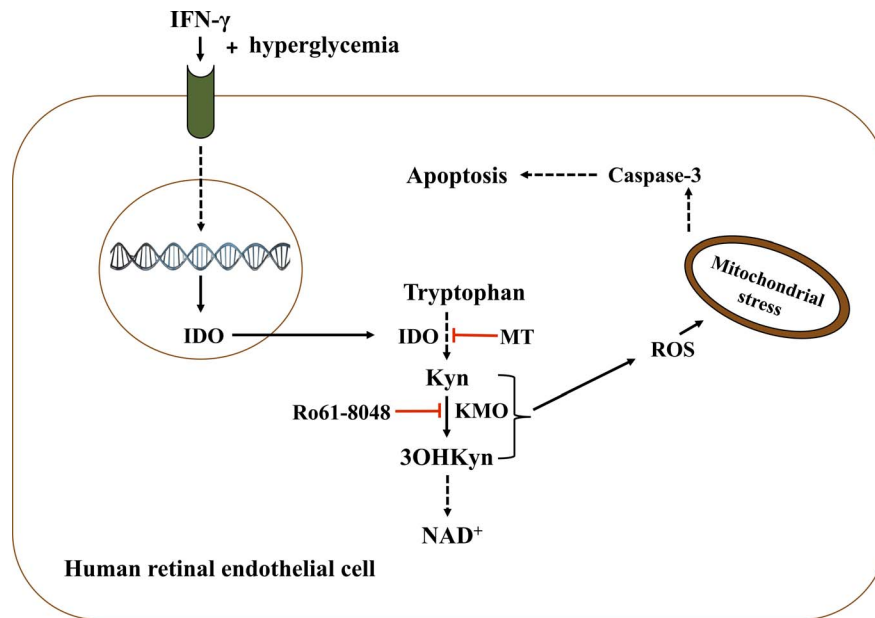
FIGURE 7. Proposed scheme for IDO-mediated retinal capillary degeneration in diabetes. IFN-γ induced the expression of IDO in HREC and this was enhanced by high glucose. IDO expression produced Kyn and 3OHKyn that led to the formation of ROS and apoptosis of cells.

Ro61-8048 in the presence of IFN-γ and high glucose significantly reduced ROS and improved viability of HREC. The cell-permeable ROS scavenger TEMPOL also reduced the number of apoptotic HREC. This provides evidence that metabolites of an imbalanced Kyn pathway shift the redox balance toward a pro-oxidative state, leading to cellular apoptosis. The early appearance of apoptotic endothelial cells and acellular capillaries in diabetic retinas might result from oxidative stress caused by an imbalance in the Kyn pathway due to upregulated IDO. This also provides an alternative mechanism for the observed inhibition of retinal capillary degeneration in diabetic animals receiving anti-inflammatory therapy.[35,52,53] Additionally, the beneficial effects of antioxidant therapy on DR in experimental animals[54] could be partly due to the inhibition of ROS formation from 3OHKyn. Our group has previously shown that inflammatory cytokines downregulate Hsp27 in HREC, inducing apoptosis.[34] This could be an additional pathway for retinal endothelial cell apoptosis in diabetes.

Since IFN-γ–inducible IDO is the first and rate-limiting step of the Kyn pathway whose imbalance leads to oxidative stress and endothelial cell apoptosis, we investigated whether knocking out IDO in diabetic mice would affect the formation of retinal acellular capillaries. IDO^{−/−} diabetic mice had significantly fewer acellular capillaries when compared to WT diabetic mice and were comparable to nondiabetic mice. Figure 7 summarizes the possible events involved in IDO-mediated retinal capillary degeneration. Whether a similar mechanism contributes to retinal pericyte and ganglion cell apoptosis is yet to be determined.[55,56] Kyn acts as an endothelium-derived relaxing factor and promotes vasodilation,[57] suggesting that IDO might also play a role in retinal vascular regulation. Several pharmacologic agents are available for inhibition of IDO and KMO. Whether those agents would be protective against DR is yet to be determined.

CONCLUSIONS

In conclusion, the present study provides insights into the molecular mechanisms of diabetic endothelial cell apoptosis, wherein (1) elevated IFN-γ induces IDO in the retinal capillary endothelium, (2) hyperglycemia potentiates IFN-γ–mediated IDO expression, (3) oxidative stress plays a vital role in IDO-mediated endothelial cell apoptosis, and (4) the absence of IDO in diabetic mice alleviates acellular capillary formation. Our results link the Kyn pathway to early diabetic endothelial cell loss in retinal capillaries, and open a new avenue to pursue therapeutics.

References

1. Tarr JM, Kaul K, Chopra M, Kohner EM, Chibber R. Pathophysiology of diabetic retinopathy. *ISRN Ophthalmol.* 2013;2013:343560.

2. Tang J, Kern TS. Inflammation in diabetic retinopathy. *Prog Retin Eye Res.* 2011;30:343–358.

3. Gardner TW, Antonetti DA, Barber AJ, LaNoue KF, Levison SW. Diabetic retinopathy: more than meets the eye. *Surv Ophthalmol.* 2002;47(suppl 2):S253–S262.

4. Demircan N, Safran BG, Soylu M, Ozcan AA, Sizmaz S. Determination of vitreous interleukin-1 (IL-1) and tumour

necrosis factor (TNF) levels in proliferative diabetic retinopathy. *Eye (Lond)*. 2006;20:1366–1369.

5. Yuuki T, Kanda T, Kimura Y, et al. Inflammatory cytokines in vitreous fluid and serum of patients with diabetic vitreoretinopathy. *J Diabetes Complications*. 2001;15:257–259.

6. Franks WA, Limb GA, Stanford MR, et al. Cytokines in human intraocular inflammation. *Curr Eye Res*. 1992;11(suppl):187–191.

7. Pavan J, Salopek-Rabatic J, Kastelan S, Jukic A, Vickovic K. Quantification of intraocular IFNgamma and IgG in cataract and diabetes. *Coll Antropol*. 2013;37(suppl 1):97–102.

8. Gustavsson C, Agardh E, Bengtsson B, Agardh CD. TNF-alpha is an independent serum marker for proliferative retinopathy in type 1 diabetic patients. *J Diabetes Complications*. 2008; 22:309–316.

9. Klein BE, Knudtson MD, Tsai MY, Klein R. The relation of markers of inflammation and endothelial dysfunction to the prevalence and progression of diabetic retinopathy: Wisconsin epidemiologic study of diabetic retinopathy. *Arch Ophthalmol*. 2009;127:1175–1182.

10. Dong N, Xu B, Wang B, Chu L. Study of 27 aqueous humor cytokines in patients with type 2 diabetes with or without retinopathy. *Mol Vis*. 2013;19:1734–1746.

11. Valverde AM, Miranda S, Garcia-Ramirez M, Gonzalez-Rodriguez A, Hernandez C, Simo R. Proapoptotic and survival signaling in the neuroretina at early stages of diabetic retinopathy. *Mol Vis*. 2013;19:47–53.

12. Mizutani M, Kern TS, Lorenzi M. Accelerated death of retinal microvascular cells in human and experimental diabetic retinopathy. *J Clin Invest*. 1996;97:2883–2890.

13. Veenstra AA, Tang J, Kern TS. Antagonism of CD11b with neutrophil inhibitory factor (NIF) inhibits vascular lesions in diabetic retinopathy. *PLoS One*. 2013;8:e78405.

14. Wallet MA, Wallet SM, Guiulfo G, Sleasman JW, Goodenow MM. IFNgamma primes macrophages for inflammatory activation by high molecular weight hyaluronan. *Cell Immunol*. 2010;262:84–88.

15. Johnson-Leger C, Hasbold J, Holman M, Klaus GG. The effects of IFN-gamma on CD40-mediated activation of B cells from X-linked immunodeficient or normal mice. *J Immunol*. 1997; 159:1150–1159.

16. Tewari K, Nakayama Y, Suresh M. Role of direct effects of IFN-gamma on T cells in the regulation of CD8 T cell homeostasis. *J Immunol*. 2007;179:2115–2125.

17. Hooks JJ, Chan CC, Detrick B. Identification of the lymphokines, interferon-gamma and interleukin-2, in inflammatory eye diseases. *Invest Ophthalmol Vis Sci*. 1988;29:1444–1451.

18. Limb GA, Little BC, Meager A, et al. Cytokines in proliferative vitreoretinopathy. *Eye (Lond)*. 1991;5(pt 6):686–693.

19. Knol JA, van Kooij B, de Valk HW, Rothova A. Rapid progression of diabetic retinopathy in eyes with posterior uveitis. *Am J Ophthalmol*. 2006;141:409–412.

20. Egwuagu CE. Chronic intraocular inflammation and development of retinal degenerative disease. *Adv Exp Med Biol*. 2014; 801:417–425.

21. Maheshwari RK, Srikantan V, Bhartiya D, Kleinman HK, Grant DS. Differential effects of interferon gamma and alpha on in vitro model of angiogenesis. *J Cell Physiol*. 1991;146:164–169.

22. Fathallah-Shaykh HM, Zhao LJ, Kafrouni AI, Smith GM, Forman J. Gene transfer of IFN-gamma into established brain tumors represses growth by antiangiogenesis. *J Immunol*. 2000;164: 217–222.

23. Taylor MW, Feng GS. Relationship between interferon-gamma, indoleamine 2,3-dioxygenase, and tryptophan catabolism. *FASEB J*. 1991;5:2516–2522.

24. Pfefferkorn ER, Rebhun S, Eckel M. Characterization of an indoleamine 2,3-dioxygenase induced by gamma-interferon in cultured human fibroblasts. *J Interferon Res*. 1986;6:267–279.

25. Thomas SR, Salahifar H, Mashima R, Hunt NH, Richardson DR, Stocker R. Antioxidants inhibit indoleamine 2,3-dioxygenase in IFN-gamma-activated human macrophages: posttranslational regulation by pyrrolidine dithiocarbamate. *J Immunol*. 2001;166:6332–6340.

26. Litzenburger UM, Opitz CA, Sahm F, et al. Constitutive IDO expression in human cancer is sustained by an autocrine signaling loop involving IL-6, STAT3 and the AHR. *Oncotarget*. 2014;5:1038–1051.

27. Chen Y, Guillemin GJ. Kynurenine pathway metabolites in humans: disease and healthy states. *Int J Tryptophan Res*. 2009;2:1–19.

28. King NJ, Thomas SR. Molecules in focus: indoleamine 2,3-dioxygenase. *Int J Biochem Cell Biol*. 2007;39:2167–2172.

29. Amaral M, Levy C, Heyes DJ, et al. Structural basis of kynurenine 3-monooxygenase inhibition. *Nature*. 2013;496: 382–385.

30. Fallarino F, Grohmann U, Vacca C, et al. T cell apoptosis by kynurenines. *Adv Exp Med Biol*. 2003;527:183–190.

31. Mailankot M, Smith D, Howell S, et al. Cell cycle arrest by kynurenine in lens epithelial cells. *Invest Ophthalmol Vis Sci*. 2008;49:5466–5475.

32. Mailankot M, Nagaraj RH. Induction of indoleamine 2,3-dioxygenase by interferon-gamma in human lens epithelial cells: apoptosis through the formation of 3-hydroxykynurenine. *Int J Biochem Cell Biol*. 2010;42:1446–1454.

33. Hu P, Hunt NH, Arfuso F, et al. Increased indoleamine 2,3-dioxygenase and quinolinic acid expression in microglia and Muller cells of diabetic human and rodent retina. *Invest Ophthalmol Vis Sci*. 2017;58:5043–5055.

34. Nahomi RB, Palmer A, Green KM, Fort PE, Nagaraj RH. Pro-inflammatory cytokines downregulate Hsp27 and cause apoptosis of human retinal capillary endothelial cells. *Biochim Biophys Acta*. 2014;1842:164–174.

35. Tang J, Du Y, Petrash JM, Sheibani N, Kern TS. Deletion of aldose reductase from mice inhibits diabetes-induced retinal capillary degeneration and superoxide generation. *PLoS One*. 2013;8:e62081.

36. Okuda S, Nishiyama N, Saito H, Katsuki H. 3-Hydroxykynurenine, an endogenous oxidative stress generator, causes neuronal cell death with apoptotic features and region selectivity. *J Neurochem*. 1998;70:299–307.

37. Lee MW, Park SC, Chae HS, et al. The protective role of HSP90 against 3-hydroxykynurenine-induced neuronal apoptosis. *Biochem Biophys Res Commun*. 2001;284:261–267.

38. Chatterjee PK, Cuzzocrea S, Brown PA, et al. Tempol, a membrane-permeable radical scavenger, reduces oxidant stress-mediated renal dysfunction and injury in the rat. *Kidney Int*. 2000;58:658–673.

39. Miyamoto K, Khosrof S, Bursell SE, et al. Prevention of leukostasis and vascular leakage in streptozotocin-induced diabetic retinopathy via intercellular adhesion molecule-1 inhibition. *Proc Natl Acad Sci U S A*. 1999;96:10836–10841.

40. Zeng HY, Green WR, Tso MO. Microglial activation in human diabetic retinopathy. *Arch Ophthalmol*. 2008;126:227–232.

41. Kawanokuchi J, Mizuno T, Takeuchi H, et al. Production of interferon-gamma by microglia. *Mult Scler*. 2006;12:558–564.

42. Suzuki Y, Claflin J, Wang X, Lengi A, Kikuchi T. Microglia and macrophages as innate producers of interferon-gamma in the brain following infection with Toxoplasma gondii. *Int J Parasitol*. 2005;35:83–90.

43. Sumarac-Dumanovic M, Jeremic D, Pantovic A, et al. Therapeutic improvement of glucoregulation in newly

diagnosed type 2 diabetes patients is associated with a reduction of IL-17 levels. *Immunobiology*. 2013;218:1113–1118.

44. Vujosevic S, Micera A, Bini S, Berton M, Esposito G, Midena E. Proteome analysis of retinal glia cells-related inflammatory cytokines in the aqueous humour of diabetic patients. *Acta Ophthalmol*. 2016;94:56–64.

45. Johnsen-Soriano S, Sancho-Tello M, Arnal E, et al. IL-2 and IFN-gamma in the retina of diabetic rats. *Graefes Arch Clin Exp Ophthalmol*. 2010;248:985–990.

46. O'Connor JC, Andre C, Wang Y, et al. Interferon-gamma and tumor necrosis factor-alpha mediate the upregulation of indoleamine 2,3-dioxygenase and the induction of depressive-like behavior in mice in response to bacillus Calmette-Guerin. *J Neurosci*. 2009;29:4200–4209.

47. Babcock TA, Carlin JM. Transcriptional activation of indoleamine dioxygenase by interleukin 1 and tumor necrosis factor alpha in interferon-treated epithelial cells. *Cytokine*. 2000;12:588–594.

48. Oxenkrug GF, Turski WA, Zgrajka W, Weinstock JV, Summergrad P. Tryptophan-kynurenine metabolism and insulin resistance in hepatitis C patients. *Hepat Res Treat*. 2013; 2013:149247.

49. Okuda S, Nishiyama N, Saito H, Katsuki H. Hydrogen peroxide-mediated neuronal cell death induced by an endogenous neurotoxin, 3-hydroxykynurenine. *Proc Natl Acad Sci U S A*. 1996;93:12553–12558.

50. Eastman CL, Guilarte TR. The role of hydrogen peroxide in the in vitro cytotoxicity of 3-hydroxykynurenine. *Neurochem Res*. 1990;15:1101–1107.

51. Wang Q, Zhang M, Ding Y, et al. Activation of NAD(P)H oxidase by tryptophan-derived 3-hydroxykynurenine accelerates endothelial apoptosis and dysfunction in vivo. *Circ Res*. 2014;114:480–492.

52. Rangasamy S, McGuire PG, Das A. Diabetic retinopathy and inflammation: novel therapeutic targets. *Middle East Afr J Ophthalmol*. 2012;19:52–59.

53. Zhang W, Liu H, Rojas M, Caldwell RW, Caldwell RB. Anti-inflammatory therapy for diabetic retinopathy. *Immunotherapy*. 2011;3:609–628.

54. Kowluru RA, Tang J, Kern TS. Abnormalities of retinal metabolism in diabetes and experimental galactosemia. VII. Effect of long-term administration of antioxidants on the development of retinopathy. *Diabetes*. 2001;50:1938–1942.

55. Martin PM, Roon P, Van Ells TK, Ganapathy V, Smith SB. Death of retinal neurons in streptozotocin-induced diabetic mice. *Invest Ophthalmol Vis Sci*. 2004;45:3330–3336.

56. Kern TS, Barber AJ. Retinal ganglion cells in diabetes. *J Physiol*. 2008;586:4401–4408.

57. Wang Y, Liu H, McKenzie G, et al. Kynurenine is an endothelium-derived relaxing factor produced during inflammation. *Nat Med*. 2010;16:279–285.